ACS APPLIED MATERIALS & INTERFACES

Biological and Medical Applications of Materials and Interfaces

Molecularly Imprinted Artificial Biointerface for Enzyme-Free Glucose Transistor

Taira Kajisa, and Toshiya Sakata

ACS Appl. Mater. Interfaces, **Just Accepted Manuscript** • DOI: 10.1021/acsami.8b13317 • Publication Date (Web): 20 Sep 2018

ACS Publications

is published by the American Chemical Society. 1155 Sixteenth Street N.W., Washington, DC 20036

Molecularly Imprinted Artificial Biointerface for Enzyme-Free Glucose Transistor

Taira Kajisa[†] and Toshiya Sakata[*,‡]

[†]PROVIGATE Inc. Entrepreuneur Plaza, The University of Tokyo, 7-3-1 Hongo, Bunkyo-ku, Tokyo 113-0033, Japan

[‡]Department of Materials Science and Engineering, Graduate School of Engineering, The University of Tokyo, 7-3-1 Hongo, Bunkyo-ku, Tokyo 113-8656, Japan

*Corresponding author. E-mail: sakata@biofet.t.u-tokyo.ac.jp

CORRESPONDING AUTHOR FOOTNOTE:

Affiliation: Department of Materials Engineering, School of Engineering, The University of Tokyo, 7-3-1 Hongo, Bunkyo-ku, Tokyo 113-8656, Japan

TEL: +81-3-5841-1842; FAX: +81-3-5841-1842

Keywords

Field effect transistor; Molecularly imprinted polymer; Phenylboronic acid; Glucose; Biointerface

Abstract

A platform based on a highly selective and sensitive detection device functionalized with a well-designed artificial biointerface is required for versatile biosensors. We develop a molecularly imprinted polymer (MIP)-coated gate field-effect transistor (FET) biosensor for low-concentration-glucose detection in biological fluid samples such as tears in an enzyme-free manner. The MIP includes glucose templates (GluMIP), in which glucose binds to vinylphenylboronic acid (VPBA) in the copolymerized membrane resulting in the change in the density of molecular charges of the PBA/glucose complex. The FET biosensor can detect small biomolecules as long as biomolecular recognition events cause intrinsic changes in the density of molecular charges. As a result, the changes in the output voltage detected using the GluMIP-based FET sensor are fitted to the Langmuir adsorption isotherm equation at various concentrations of sugars, showing the low detection limit of 3 μM and the high sensitivity of 115 mV/decade from 100 μM to 4 mM glucose. On the basis of the equation, the stability constant (K_a) of PBA with glucose is calculated and found to markedly increase to K_a=1192 M^{-1}, which is higher by a factor of a few hundreds than K_a=4.6 M^{-1} obtained by nonelectrical detection methods. Moreover, the GluMIP-coated gate FET sensor shows an approximately 200-fold higher selectivity for glucose than for fructose. This is because glucose binds to PBA more selectively than fructose in the templates resulting in the generation of negative charges. The electrical properties of the MIP-coated electrode are also evaluated by measuring capacitance.

Our work suggests a new strategy of designing a platform based on the MIP-coated gate FET biosensor, which is suitable for a highly selective, sensitive, enzyme-free biosensing system.

INTRODUCTION

Low-molecular-weight biomolecules are highly recognized as significant biomarker candidates in the field of *in vitro* diagnostics (IVD).[1] For the detection of small biomolecules, conventional methods require enzymatic reactions and secondary antibodies with fluorescent dyes in immunoassays.[2-7] However, fluorescent conjugates may not be formed when the target biomolecules, that is, antigens are smaller.[8,9] Although enzymes and antibodies have been utilized in a wide range of scientific fields and their applications have been recognized as the global standard, the use of these biomacromolecules is problematic owing to their fragility, high-cost and time-consuming production, and the difficulty of quality control of their production. Therefore, an artificial and functional membrane based on a standard concept should become a platform as molecular recognition sites for small biomarkers.

Molecularly imprinted polymers (MIPs) are artificial materials that can recognize biomolecules.[10-16] Molecular imprinting is a template polymerization technique involving the copolymerization of a crosslinker and a target molecule or its derivative covalently or noncovalently bound to a functional monomer. After removing the template molecule, cavities are imprinted in the polymer matrix, which are complementary to the template molecule in shape and size and capable of template molecule recognition. Imprinted polymers show a strong

binding affinity for low-molecular-weight biomolecules such as bisphenol A[13,16] and histamine.[14] However, an optical system is mostly required to detect signals from target biomolecules, resulting in large systems, troublesome procedures, and qualitative data. Moreover, MIP membranes were used for glucose recognition by a cyclic voltammetry method. In this method, $[Fe(CN)_6]^{3-/4-}$ is mostly used as a probe for the redox reaction through the template cavities in a MIP membrane with a Au electrode in a measurement solution.[17,18] Also, a fluorescent dye is copolymerized in a MIP membrane to detect glucose.[19,20] Therefore, a signal transducer, which enables the label-free detection of biomolecules, is required to directly and quantitatively analyze small biomolecules targeted in MIP membranes.

Biologically coupled gate field-effect transistors (bio-FETs) in a miniaturized system show good performance in quantitatively detecting intrinsic biomolecular charges. The principle of bio-FETs is based on potentiometric detection on the gate, where specific binding to target biomolecules occurs accompanied by their charge changes resulting in their detection. In particular, bio-FETs can directly detect even small biomolecules as long as such biomolecules have intrinsic molecular charges. Bisphenol A was quantitatively detected by open sandwich-based FETs,[21] and MIP-coated FETs directly and electrically detected small biomolecules such as histamine and oligosaccharide.[22,23] Additionally, cellular respiration was monitored in real time as the change in the concentration of even the smallest ion, H^+, at the cell/gate nanogap interface using cell-based FETs.[24–26] Thus, the principle of detection by bio-FETs is based on the

most adequate signal translator for the direct recognition of small biomolecules selectively captured in MIPs.

Electrochemical sensors can be applied as a bioanalytical tool in IVD. Glucose sensors are widely used to monitor glucose levels in blood in diabetic mellitus patients. Most glucose sensors utilize enzymatic reactions between glucose oxidase (GOD) and glucose owing to the high selectivity, convenience, and low cost of such devises, the detection principle of which can be used to analyze glucose levels with a sensitivity of about 100 mg/dl (about 5.5 mM) in blood.[1,4,7] However, conventional glucose sensors have several disadvantages; commercially available glucose sensors require blood sampling to measure blood glucose levels, which may be painful, and their detection sensitivity is insufficient at low glucose levels in biological fluids such as tears, which can be used for noninvasive glucose measurement instead of blood samples. In fact, the glucose levels in tears are about one-hundredth to one-tenth of those in blood.[27]

On the other hand, nonenzymatic glucose sensors have been proposed by applying the equilibrium reaction of the phenylboronic acid (PBA) molecule with sugars. PBA has attracted considerable attention in the field of molecular recognition as it can form stable esters with various biomolecules containing 1,2 or 1,3 cis-diol/polyol groups, such as sugars, in aqueous systems (**Scheme S1a**).[28,29] However, PBA exhibits a lower affinity for glucose than for other mono- and di-saccharides such as fructose and sucrose. To solve this problem of lower affinity of glucose, PBA-based MIPs should be used for nonenzymatic glucose sensing. The esterification of PBA/diol is a reversible reaction, which can be controlled by adjusting the pH of the solution.

Thus, the template can easily be extracted from the polymer in the preparation of MIPs by simply adjusting the pH of the solution (**Scheme S1b)**. Moreover, in the esterification, PBA switches from a nonionic form to an anionic form (**Scheme S1a**). Hence, the change in the density of molecular charges induced by the saccharide-to-PBA binding can be detected by FET biosensors.[30,31]

In this study, we propose a glucose transistor with a well-designed artificial biointerface, namely, the glucose-template MIP-coated gate FET (GluMIP-FET), as a nonenzymatic glucose sensor. In particular, the electrical properties of the GluMIP-coated Au gate electrode were investigated by measuring capacitance, and then the detection selectivity and sensitivity of the GluMIP-coated gate FET to glucose was evaluated, focusing on the stability constant of the glucose/PBA complex

RESULTS AND DISCUSSION

Radical copolymerization of GluMIP hydrogel on Au electrode. The monomer solution, which included HEMA as the main chain monomer and VPBA as the sugar recognition monomer, was directly put onto the Au surface and copolymerized in an inert gas atmosphere. The conceptual structure of GluMIP-FET is shown in **Figure 1a**, and the hydrogel was randomly copolymerized as poly(HEMA-*ran*-DMAPM-*ran*-VPBA-*ran*-AA), as shown in **Figure 1b**. Before the copolymerization, VPBA was expected to have negative charges upon binding to glucose. Glucose molecules were washed out with an acid solution after the copolymerization,

resulting in cavities formed in the MIP. As shown in **Figure S1**, which was obtained by X-ray photoelectron spectroscopy (XPS), the composition of carbon increased, while the composition of gold was hardly found, after grafting the GluMIP hydrogel onto the Au surface. Also, the B–O stretching (1337 cm^{-1}) and the formation of boronate ester (654 cm^{-1}), which were included in the GluMIP hydrogel, were observed from the spectra obtained by attenuated total reflection-Fourier transform infrared spectroscopy (ATR-FTIR), as shown in **Figure S2**. Thus, the GluMIP hydrogel was successfully grafted on the Au gate electrode.

Phase separation was observed with the GluMIP hydrogel appearing white and the NIP hydrogel maintaining its transparency (**Figure S3**). This may be because the hydrophilic monomer, which is VPBA that became charged upon its binding to glucose, was phase-separated with the hydrophobic monomers in GluMIP, whereas the NIP hydrogel was copolymerized by the uncharged monomers.

Capacitance characteristic of GluMIP hydrogel interface. After polymerizing and removing the glucose template, the capacitance of the GluMIP hydrogel on the Au electrode were evaluated using an LCR meter. **Figure 2** shows the changes in the capacitance of the GluMIP hydrogel (ΔC_{GluMIP}) at each concentration of glucose. The permittivity of the GluMIP hydrogel depends on the bias voltage; therefore, ΔC_{GluMIP} was monitored in real-time at 200 Hz frequency and 0 V at various glucose concentrations. The data are plotted in **Figure 2** as the averages of capacitances monitored for 20 min at each glucose concentration, with the standard errors shown. As a result, C_{GluMIP} increased with increasing glucose concentration, which means that the

GluMIP hydrogel swelled owing to the increase in the density of negative charges based on the glucose/PBA complexes. However, ΔC_{GluMIP} of the GluMIP hydrogel at various glucose concentrations was not very large, compared with that of the hydrophobic polymer.[32,33] The MIP hydrogel used in this study included HEMA as the main chain monomer, which is a hydrophilic polymer even before adding glucose. This is the reason why the MIP hydrogel basically included a large number of water molecules, that is, the change in the permittivity of the MIP hydrogel was almost negligible even after adding glucose. This is also because the crosslink density in the GluMIP was higher in this study than in our previous study.[31] Therefore, the swelling rate of the GluMIP hydrogel was relatively low owing to its intrinsic hydrophilic property and relatively high crosslink density.

Electrical characteristics of GluMIP-coated gate FET. The pH and glucose responsivities of the GluMIP-coated gate FET was investigated using a semiconductor parameter analyzer. In this case, no glucose was introduced into the GluMIP hydrogel. **Figure 3** shows the changes in V_G from pH 6 to 12 at I_D of 1 mA and V_D of 2.5 V, which was analyzed from the V_G-I_D electrical characteristics obtained in 100 mM sodium phosphate buffers with different pHs. The plotted data were fitted by the Sigmoid function described as

$$y = (a-d)/[1+(x/c)^b] - d, \quad (1)$$

where a is the minimum V_G, b is defined as the Hill coefficient, c is the pK_a, and d is the maximum V_G. V_G shifted from -394 to -294 mV within pHs 6 to 12. PBA in the GluMIP without glucose keeps the equilibrium reaction between states 1 and 2 (**Scheme S1a**), depending on the

pH. The FET can detect the change in the molecular charges on basis of the equilibrium state of PBA at various pHs. In addition, the inflection point in the Sigmoid curve is represented as pK_a; thus, pK_a was determined as 9.2 using the GluMIP-coated gate FET, although the pK_a of PBA was in the range from 8.6 to 8.8 in previous works.[34-36] This may be due to the measurement system and its environment. That is, the equilibrium state based on microenvironmental pH in the GluMIP around the gate/solution interface is different from that in the bulk solutions. The most rigorous molecular dynamics simulations have demonstrated that counter ions form 2-3 layers accompanied by an electrostatic interaction with polarized water molecules at the substrate/solution interface, where the type of interaction depends on ionic strength, different from that in a bulk solution.[37-40]

Moreover, glucose responsivity of the GluMIP-coated gate FET was analyzed from the V_G-I_D electrical characteristics. **Figure 4** shows ΔV_T analyzed from the V_G-I_D electrical characteristics of the GluMIP-coated gate FETs at various glucose concentrations. ΔV_T shifted in the positive direction at I_D of 1 mA with increasing glucose concentration from 10 μM to 10 mM. The positive shift of ΔV_T means the increase of negative charges at the gate of FET devices; therefore, the increase of negative charges caused by the formation of the glucose/PBA complex was detected using the GluMIP-coated gate FET, on the basis of the increase in glucose concentration. In a previous report, the V_G-I_D electrical characteristics were evaluated using the stimulus responsive polymer-gel-modified glucose FET sensor.[32] In this case, ΔV_T shifted in the negative direction after the addition of 5 g/L glucose, which was opposite to our results. This is because

the previous work demonstrated the change in the capacitance of the gel, which was based on the deswelling to swelling of the polymer gel. That is, the change in capacitance as the output was largely determined using FET devices, although the change in the molecular charges of the gel was slightly included in the output signal, in the previous work. In this study, the capacitance of the GluMIP hydrogel hardly changed after adding glucose (**Figure 2**); therefore, the increase in negative charges based on the formation of the glucose/PBA complex was detected as larger signals on the basis of the principle of the field effect than that resulting from the swelling of the GluMIP hydrogel after glucose addition.

Glucose monitoring with GluMIP-FET. Figure 5 shows ΔV_{out} to various saccharides detected using the GluMIP-FET. Glucose, fructose, and sucrose at 1 mM were added onto the GluMIP-coated Au gate electrode. Each sugar was added onto an identical electrode in turn to examine the potential responsivity to sugars and the selectivity to glucose detected using the GluMIP-FET. ΔV_{out} is obtained as the change in source-gate voltage (ΔV_{GS}) through the source follower circuit, which corresponds to $-\Delta V_T$. As a result, ΔV_{out} hardly changed upon adding fructose or sucrose, but shifted in the negative direction by about 100 mV upon adding glucose. The negative shift in V_{out} resulted from the negative charges of the glucose/PBA complex formed in the GluMIP hydrogel. Thus, the GluMIP-FET enabled the selective detection of glucose. Moreover, **Figure 6** shows ΔV_{out} of the GluMIP-FET with the change in the concentration of each sugar. ΔV_{out} clearly decreased upon adding glucose from 10 μM to 20 mM, while other sensors did not respond upon adding each sugar. In particular, ΔV_{out} for the NIP-FET shifted in the positive

direction upon adding glucose, although the signal shifts were very small. The positive shifts would be due to the increase in the capacitance of NIP, because the swelling of NIP was induced upon the addition of glucose solutions, resulting in the increase in the permittivity of NIP. This means that the response of the GluMIP-FET to glucose may slightly include the change in the capacitance of the polymer, although the signal contamination is assumed to be small. Note that NIP did not have the glucose template supported by PBA but it included PBA. Thus, the change in the shape of the MIP membrane depending on its swelling/deswelling was not so large owing to the more dense crosslinking, which prevented more water molecules from invading into the MIP hydrogel. However, the GluMIP-FET detected the increase in the density of negative charges on the basis of the glucose/PBA complexes with high sensitivity.

To analyze the binding affinity and kinetics of the GluMIP-FET for each sugar, ΔV_{out} values of GluMIP-FETs were plotted against the change in the concentration of each sugar in **Figure 7** on the basis of the data obtained in **Figure 6**. These analyzed curves seem to be approximated by the Langmuir adsorption isotherm. As shown by the equilibrium reaction between PBA and a diol compound such as sugars in **Scheme S1a**, the FET devices can detect molecular charges of tetrahedral PBAs, which maintain the equilibrium reaction with noncharged trigonal PBAs. The binding affinity of PBA for diol is pH-dependent, and it is generally understood that the $VPB(OH)_3^-$ complex is considerably more stable than the $VPB(OH)_2$ complex;[36] therefore, the equilibrium reaction between PBA and sugar can be represented as,

$$[PBA]_{non-charged} + [sugar] \leftrightarrows [PBA - sugar]_{charged} \ . \ (2)$$

According to equation (2), the binding constant (K_a) and the law of conservation of mass can be represented as

$$K_a = \frac{[PBA-sugar]_{charged}}{[PBA]_{non-charged}[sugar]}, (3)$$

$$[PBA-sugar]_{charged} + [PBA]_{non-charged} = [PBA-sugar]^{max}_{charged}, (4)$$

where $[PBA-sugar]^{max}_{charged}$ indicates the maximum concentration of the charged PBA-sugar conjugate, corresponding to the total number of charged PBA molecules with diol binding to sugar. Considering equations (2) to (4), ΔV_{out} based on the equilibrium reaction is approximated to the Langmuir adsorption isotherm as

$$\frac{[PBA-sugar]_{charged}}{[PBA-sugar]^{max}_{charged}} = \frac{[sugar]}{\frac{1}{K_a}+[sugar]} = \frac{\Delta V_{out}}{\Delta V^{max}_{out}}$$

$$\rightarrow \Delta V_{out} = \frac{\Delta V^{max}_{out}\,[sugar]}{\frac{1}{K_a}+[sugar]}, (5)$$

where ΔV^{max}_{out} indicates the maximum ΔV_{out} saturated at higher concentrations of sugar, which is analyzed from **Figure 7**. Note that the change in the concentration of sugar ($[sugar]$) contributes to the change in the charge of the PBA/sugar complex (ΔQ_{co}) in the GluMIP hydrogel, as shown in our previous work.[23] ΔV_{out} is basically calculated on the basis of ΔQ_{co} at a constant capacitance ($\Delta C_{GluMIP} \approx 0$). Considering our previous work,[23] ΔV_{out} can be evaluated on the basis of ΔQ_{co}, that is, $[sugar]$, when ΔC_{GluMIP} is almost negligible in terms of the change in the concentration of sugar. In fact, ΔC_{GluMIP} hardly changed even after adding glucose (**Figure 2**); therefore, ΔV_{out} can be related to $[sugar]$ as equation (5). According to equation (5), K_a and the decision coefficients (R^2) of the fitting curve to each sugar concentration were calculated from the data shown in **Figure 7**, as shown in **Table 1**. Considering the calculated data of R^2,

ΔV_{out} of the GluMIP-FETs well fitted to the Langmuir plots for each sugar concentration. Moreover, K_a obtained in this study was much higher than that previously reported,[28] where the K_a values for the competitive reaction of sugars with Arizarin Red S (ARS) in terms of PBA molecules in a buffer solution (pH 7.4) were calculated to be 4.6 M^{-1} for glucose, 160 M^{-1} for fructose, and 0.67 M^{-1} for sucrose without using MIPs. Thus, K_a for glucose (1192 M^{-1}) detected using the GluMIP-FET was approximately 250 times higher than that (4.6 M^{-1}) previously reported. Furthermore, the detection selectivity of glucose to fructose or sucrose ($S_{glu/fru}$ or $S_{glu/suc}$) is defined by K_a as

$$S_{glu/sugar} = \frac{K_a \; for \; glucose}{K_a \; for \; sugar} \quad . (6)$$

$S_{glu/fru}$ and $S_{glu/scu}$ in this study were calculated to be 5.6 and 4.4, and those in Ref. 25 were 0.029 and 6.9, respectively. From these calculations, the detection selectivity of glucose to fructose using the GluMIP-FET was about 200 times higher than that in previous methods. However, the detection selectivity of glucose to sucrose was almost unchanged even when using the GluMIP-FET. This is because sucrose is a disaccharide composed of the monosaccharides glucose and fructose; therefore, the GluMIP-FET may have recognized the glucose structure in sucrose. Nevertheless, this does not mean that the detection selectivity of glucose to sucrose with the PBA-diol binding has been lost when using the GluMIP-FET. Thus, the well-designed artificial MIP interface is very effective for increasing not only the binding constant but also the detection selectivity for low-molecular-weight biomolecules, because the FET device can directly detect molecular charges. Moreover, **Figure 7b** shows ΔV_{out} for the base 10 logarithm of sugar

concentrations on the basis of the data shown in **Figure 7a**. The detection sensitivities of the GluMIP-FET to the sugars in the range of 100 μM to 4 mM were 114.8 mV/decade for glucose, 8.6 mV/decade for fructose, and 5.1 mV/decade for sucrose, respectively. Thus, the detection sensitivity to glucose was about 15 to 20 times higher than those to other sugars owing to the well-designed artificial MIP interface that provided the glucose specificity. Moreover, the limit of detection (LOD) for glucose using the GluMIP-FET in this study was predicted to be about 3 μM from the semilogarithmic plots, on the basis of the Kaiser limit theory.[41] Therefore, the GluMIP-FET can detect glucose at a low concentration in biological fluids such as tears, where the glucose levels are about one-hundredth to one-tenth of those in blood.[27] Thus, the well-designed artificial MIP interface is very effective for increasing not only the binding constant but also the detection selectivity for low-molecular-weight biomolecules, which results from the FET device enabling the direct detection of molecular charges.

Generally, FET biosensors can detect molecular charges within the Debye length (diffusion layer) at the electrolyte/gate interface. The LOD of FET biosensors depends on the Debye length,[42-44] as expressed by

$$\lambda = \sqrt{\frac{\varepsilon_0 \varepsilon_r k_B T}{2 N_A e^2 I}}, \quad (7)$$

where I is the ionic strength of an electrolyte, ε_0 is the permittivity of free space, ε_r is the dielectric constant, k_B is the Boltzmann constant, T is the absolute temperature, N_A is the Avogadro number, and e is the elementary charge.[45] For example, the Debye length is calculated to be 0.75 nm even in a 150 mM NaCl solution. This is why the Debye length would be about 1

nm at most in this study, where 100 mM sodium phosphate buffer was used as the measurement solution. Therefore, the change in the molecular charges of the glucose/PBA complex formed inside the GluMIP-coated gate, which was in the vicinity of Au surface, namely, in the diffusion layer, should have been detected using the potentiometric sensor, owing to the hydrophilic polymer interface. Although the thickness of the GluMIP membrane was about 200 nm, which was measured using a mechanical profilometer (**Figure S4**), and not precisely controlled in this study, the effect of the thickness of the polymer interface on the performances of FET biosensors will be investigated by controlling the thickness and examined focusing on the Debye length. In this case, surface-initiated atom transfer radical polymerization (SI-ATRP) allows the formation of a MIP interface with a well-defined densely packed structure on a substrate, whose thickness is precisely controlled.[46,47] Thus, the well-defined polymer film, whose thickness is precisely controlled by SI-ATRP, contributes to the quantitative detection of signals by FET biosensors and provides valuable information for the fabrication of novel bioanalytical devices.

EXPERIMENTAL METHODS

Materials. As monomers in MIP polymerization, 2-hydroxyethylmethacrylate (HEMA, MW=130.14) and 4-vinylphenylboronic acid (VPBA, MW=147.97) were purchased from Tokyo Chemical Industries (Japan), and *N*-3-(dimethylamino) propylmethacrylamide (DMAPM, MW=170.25), *N,N*-methylenebisacrylamide (MBA, MW=154.17) and acrylic acid (AA, MW=72.06) were obtained from Wako Pure Chemical (Japan). AA was neutralized to pH 6.5

with 1 M NaOH and used at approximately 6.5 % (wt/wt) in the reaction solution. Copolymerization was initiated with a potassium persulfate (KPS, Wako Pure Chemical Ltd.) and tetramethylethylenediamine (TEMED, Wako Pure Chemical Ltd). As samples, glucose, fructose, and sucrose were selected for electrical measurements (Wako Pure Chemical Ltd). Ultrapure water (Ul-pure, Komatsu Electronics Co., Ltd.) was used in all experiments.

Coating of GluMIP hydrogel on Au gate surface. A Au thin film with a thickness of 100 nm/15 nm was sputtered on a white cut glass slide (Matsunami Glass Ind., Ltd.). A Ti layer was utilized as the adhesive layer between the Au film and the glass slide. A transparent polycarbonate ring (inner diameter of 18 mm/outer diameter of 20 mm) was encapsulated on the Au thin film using an epoxy resin (ZC-203T, Pelnox Ltd., Japan) except for the sensing surface. The Au substrate was cleaned using a UV ozone cleaner (MEIWAFOSIS Co., Ltd., Japan) for 60 min following immersion in Piranha solution (30 % vol. H_2O_2/H_2SO_4=3:7 by volume) for 5 min to remove organic compounds. The glucose-imprinted hydrogel was copolymerized onto the Au substrate. A monomer solution was prepared as follows: HEMA (0.20 g), DMAPM (0.10 g), VPBA (0.02 g), MBA (0.02 g), and glucose as the template (0.01 g) were diluted with deionized water to form solutions with a weight of 1.0 g including 6.5 % (wt/wt) AA. The monomer solution was agitated with a vortex mixer and degassed by bubbling nitrogen for 30 min. After degassing, the monomer solution was placed on ice; into the solution, 2 μl of TEMED and 5 μl of KPS solution (50 mg/ml) was mixed by gently pipetting. Polymerization was initiated by

pouring 5 μl of the monomer solution on the Au surface, which was covered with a polyethylene terephthalate (PET) film, and was then polymerized overnight in a desiccator in nitrogen atmosphere. After copolymerization, the PET film was peeled off, and then template-glucose molecules and remaining monomers were washed by immersing the substrate in 0.05 M HCl/50% vol. methanol solution and then with ultrapure water. The prepared MIP gel was equilibrated in 100 mM sodium phosphate buffer (pH 9.0) before electrochemical measurements. On the other hand, a non-imprinted polymer (NIP) was prepared on the Au substrate as a control polymer, which was prepared by the same method as that for MIP except for adding glucose as the template.

Capacitance measurement with GluMIP-coated Au electrode. To electrochemically analyze GluMIP coated on the Au electrode, the changes in capacitance were measured at various glucose concentrations from 10 μM to 10 mM. Capacitance was measured using an LCR meter (E4980A, Keysight technologies) at a frequency of 200 kHz and a bias voltage of 0 V. Sodium phosphate buffer at 100 mM (pH 9.0) was used for the measurements, which was connected with a Ag/AgCl reference electrode in the saturated KCl solution through an agar-based salt bridge.

Electrical measurement of sugar response using GluMIP-coated gate FET. In this study, an extended-gate FET was used to measure sugar responses, the GluMIP-coated Au electrode of which was extended from the gate of a junction FET (Toshiba), as shown **Figure 1**. A shift of the threshold voltage (ΔV_T) was measured at a drain current (I_D) of 1 mA and drain voltage (V_D) of 2.5 V in 100 mM sodium phosphate buffer (pH 9.0) at room temperature using a semiconductor

parameter analyzer (B1500A, Keysight Technologies). To measure the pH titration curve, gate voltage (V_G)-I_D electrical characteristics were measured at various pHs from 6 to 12, and then ΔV_G at 1 mA of I_D was plotted as ΔV_T at various pHs. Moreover, changes in the surface potential (ΔV_{out}) of the GluMIP-coated Au electrode were measured in real time using a source follower circuit,[48] as shown in **Figure S5**, where the Ag/AgCl reference electrode with the saturated KCl solution (3.3 M), which was connected to a measurement solution through a salt bridge, was maintained at 0 V by connecting to the ground. Electrical measurements were performed at constant I_D of 700 μA and V_D of 2 V. 1.5 ml of 100 mM sodium phosphate buffer (pH 9.0) was poured into the chemically modified Au gate surface surrounded by a 20-mm-diameter polycarbonate ring. After the stabilization of V_{out}, titrated solutions of each sugar from 5 μM to 20 mM were prepared in the buffer solution. To suppress background noises generated during the sample addition, the volume of a sample solution added was determined to be 1/100 of the total volume of the measurement solution.

CONCLUSIONS

In this study, we developed a MIP-coated gate FET biosensor for a low-level-glucose detection in biological fluid samples such as tears in an enzyme-free manner. The MIP included glucose templates (GluMIP), in which glucose bound to VPBA in the copolymerized membrane resulting in the change in the molecular charge of the PBA/glucose complex. The FET biosensor has an advantage in that it enables the detection of small biomolecules as long as biomolecular

recognition events cause changes in the density of intrinsic molecular charges. As a result, the changes in the output voltage detected using the GluMIP-based FET sensor were fitted to the Langmuir adsorption isotherm equation at various concentrations of sugars, showing the low detection limit of 3 μM and the high sensitivity of 115 mV/decade from 100 μM to 4 mM glucose. On the basis of the equation, the stability constant (K_a) of PBA with glucose was calculated and found to remarkably increase to K_a=1192 M^{-1}, which was higher by a factor of a few hundreds than K_a=4.6 M^{-1} obtained by nonelectrical detection methods. Moreover, the GluMIP-coated gate FET sensor showed an approximately 200-fold higher selectivity for glucose than for fructose. This is because glucose bound to PBA more selectively than fructose in the templates resulting in the generation of negative charges. The electrical properties of the MIP-coated electrode were also evaluated by measuring capacitance. Our work suggests a new strategy of designing a platform based on the MIP-coated gate FET biosensor, which is suitable for a highly selective, sensitive, enzyme-free biosensing system.

ASSOCIATED CONTENT

Supporting Information

The Supporting Information is available free of charge on the ACS Publications website at DOI:***. Schematic illustration of molecularly imprinted polymer (MIP) with phenylboronic

acid (PBA) (**Scheme S1**); XPS spectra for C 1s and Au 4f5/2, 4f7/2 (**Figure S1**); ATR-FTIR spectra of Au and GluMIP-coated Au electrodes (**Figure S2**); Image of copolymerized hydrogels (**Figure S3**); Thickness profile of GluMIP-coated Au obtained using the stylus-type profiler (**Figure S4**); Source follower circuit for real-time FET measurement system (**Figure S5**).

AUTHOR INFORMATION

Corresponding Author

*E-mail: sakata@biofet.t.u-tokyo.ac.jp

CORRESPONDING AUTHOR FOOTNOTE: Affiliation; Department of Materials Engineering, School of Engineering, The University of Tokyo, 7-3-1 Hongo, Bunkyo-ku, Tokyo113-8656, Tokyo

ORCID

Taira Kajisa: 0000-0001-6121-9274

Toshiya Sakata: 0000-0003-1246-5000

Notes

The authors declare no competing financial interest.

ACKNOWLEDGMENTS

Part of this study was supported by the Program for Creating STart-ups from Advanced Research and Technology (START program) promoted by the Ministry of Education, Culture, Sports, Science and Technology, Japan.

REFERENCES

(1) Updike, S. J.; Hicks, G. P. The Enzyme Electrode. *Nature* **1967**, *214*, 986–988.

(2) Coons, A. H. C., H. J.; Jones, R. N.; Berliner, E. The Demonstration of Pneumococcal Antigen in Tissues by the Use of Fluorescent Antibody. *J. Immunol.* **1942**, *45*, 159–170.

(3) Engvall, E.; Perlmann, P. Enzyme-Linked Immunosorbent Assay (Elisa). Quantitative Assay of Immunoglobulin G. *Immunochem.* **1971**, *8*, 871–874.

(4) Suckling, C. J. Immobilized Enzymes. *Chem. Soc. Rev.* **1977**, *6*, 215–233.

(5) Palomäki, P. Simultaneous Use of Poly- and Monoclonal Antibodies as Enzyme Tracers in a One-Step Enzyme Immunoassay for the Detection of Hepatitis B Surface Antigen. *J. Immunol. Methods* **1991**, *145*, 55–63.

(6) Rao, P. N.; Taraporewala, I. B. A Sensitive Enzyme-Linked Immunosorbent Assay (Elisa) for Testosterone: Use of a Novel Heterologous Hapten Conjugated to Penicillinase. *Steroids* **1992**, *57*, 154–161.

(7) Newman, J. D.; Turner, A. P. Home Blood Glucose Biosensors: A Commercial Perspective. *Biosens. Bioelectron.* **2005**, *20*, 2435–2453.

(8) Ueda, H.; Tsumoto, K.; Kubota, K.; Suzuki, E.; Nagamune, T.; Nishimura, H.; Schueler, P. A.; Winter, G.; Kumagai, I.; Mohoney, W. C. Open Sandwich Elisa: A Novel Immunoassay Based on the Interchain Interaction of Antibody Variable Region. *Nat. Biotechnol.* **1996**, *14*, 1714–1718.

(9) Suzuki, C.; Ueda, H.; Mahoney, W.; Nagamune, T. Open Sandwich Enzyme-Linked Immunosorbent Assay for the Quantitation of Small Haptens. *Anal. Biochem.* **2000**, *286*, 238–246.

(10) Wulff, G.; Schauhoff, S. Enzyme-Analog-Built Polymers. 27. Racemic Resolution of Free Sugars with Macroporous Polymers Prepared by Molecular Imprinting. Selectivity Dependence on the Arrangement of Functional Groups Versus Spatial Requirements. *J. Org. Chem.* **1991**, *56*, 395–400.

(11) Wulff, G. Molecular Imprinting in Cross-Linked Materials with the Aid of Molecular Templates - a Way Towards Artificial Antibodies. *Angewandte Chemie-International Edition in English* **1995**, *34*, 1812–1832.

(12) Takeuchi, T.; Matsui, J. Molecular Imprinting: An Approach to "Tailor-Made" Synthetic Polymers with Biomimetic Functions. *Acta Polym.* **1996**, *47*, 471–480.

(13) Lee, W.-S.; Takeuchi, T. Bisphenol a Analog-Imprinted Polymers Prepared by an Immobilized Template on a Modified Silica Microsphere Matrix. *Anal. Sci.* **2005**, *21*, 1125–1128.

(14) Horemans, F.; Alenus, J.; Bongaers, E.; Weustenraed, A.; Thoelen, R.; Duchateau, J.; Lutsen, L.; Vanderzande, D.; Wagner, P.; Cleij, T. J. Mip-Based Sensor Platforms for the Detection of Histamine in the Nano- and Micromolar Range in Aqueous Media. *Sens. Actuat. B.* **2010**, *148*, 392–398.

(15) Takeuchi, T.; Hayashi, T.; Ichikawa, S.; Kaji, A.; Masui, M.; Matsumoto, H.; Sasao, R. Molecularly Imprinted Tailor-Made Functional Polymer Receptors for Highly Sensitive and Selective Separation and Detection of Target Molecules. *Chromatography* **2016**, *37*, 43–64.

(16) Herrero-Hernández, E.; Carabias-Martínez, R.; Rodríguez-Gonzalo, E. Behavior of Phenols and Phenoxyacids on a Bisphenol-a Imprinted Polymer. Application for Selective

Solid-Phase Extraction from Water and Urine Samples. *Int. J. Mol. Sci.* **2011**, *12*, 3322–3339.

(17) Yang, Y.; Yi, C.; Luo, J.; Liu, R.; Liu, J.; Jiang, J.; Liu, X. Glucose Sensors Based on Electrodeposition of Molecularly Imprinted Polymeric Micelles: A Novel Strategy for MIP Sensors. *Biosens. Bioelectron.* **2011**, *26*, 2607–2612.

(18) Zhao, W.; Zhang, R.; Xu, S.; Cai, J.; Zhu, X.; Zhu, Y.; Wei, W.; Liu, X.; Luo, J. Molecularly Imprinted Polymeric Nanoparticles Decorated with Au NPs for Highly Sensitive and Selective Glucose Detection. *Biosens. Bioelectron.* **2018**, *100*, 497–503.

(19) Manju, S.; Hari, P.R.; Sreenivasan, K. Fluorescent Molecularly Imprinted Polymer Film Binds Glucose with a Concomitant Changes in Fluorescence. *Biosens. Bioelectron.* **2010**, *26*, 894–897.

(20) Wang, H.; Yi, J.; Velado, D.; Yu, Y.; Zhou, S. Immobilization of Carbon Dots in Molecularly Imprinted Microgels for Optical Sensing of Glucose at Physiological pH. *ACS Appl. Mater. Interfaces* **2015**, *7*, 15735−15745.

(21) Sakata, T.; Ihara, M.; Makino, I.; Miyahara, Y.; Ueda, H. Open Sandwich-Based Immuno-Transistor for Label-Free and Noncompetitive Detection of Low Molecular Weight Antigen. *Anal. Chem.* **2009**, *81*, 7532–7537.

(22) Yang, H.; Nishitani, S.; Sakata, T. Potentiometric Langmuir Isotherm Analysis of Histamine-Selective Molecularly Imprinted Polymer-Based Field-Effect Transistor. *ECS J. Solid State Sci. Technol.* **2018**, *7*, Q3079–Q3082.

(23) Nishitani, S.; Sakata, T. Potentiometric Adsorption Isotherm Analysis of a Molecularly Imprinted Polymer Interface for Small-Biomolecule Recognition. *ACS Omega* **2018**, *3*, 5382–5389.

(24) Sakata, T.; Saito, A.; Mizuno, J.; Sugimoto, H.; Noguchi, K.; Kikuchi, E.; Inui, H. Single Embryo-Coupled Gate Field Effect Transistor for Elective Single Embryo Transfer. *Anal. Chem.* **2013**, *85*, 6633–6638.

(25) Izak, T.; Krátká, M.; Kromka, A.; Rezek, B. Osteoblastic Cells Trigger Gate Currents on Nanocrystalline Diamond Transistor. *Colloids Surf. B. Biointerfaces* **2015**, *129*, 95–99.

(26) Satake, H.; Saito, A.; Sakata, T. Elucidation of Interfacial Ph Behaviour at the Cell/Substrate Nanogap for in Situ Monitoring of Cellular Respiration. *Nanoscale* **2018**, *10*, 10130–10136.

(27) Moyer, J.; Wilson, D.; Finkelshtein, I.; Wong, B.; Potts, R. Correlation between Sweat Glucose and Blood Glucose in Subjects with Diabetes. *Diabetes Technol. Ther.* **2012**, *14*, 398–402.

(28) Springsteen, G.; Wang, B. A Detailed Examination of Boronic Acid–Diol Complexation. *Tetrahedron* **2002**, *58*, 5291–5300.

(29) Yang, W.; Gao, X.; Wang, B. Boronic Acid Compounds as Potential Pharmaceutical Agents. *Med. Res. Rev.* **2003**, *23*, 346–368.

(30) Kajisa, T.; Sakata, T. Fundamental Properties of Phenylboronic-Acid-Coated Gate Field-Effect Transistor for Saccharide Sensing. *ChemElectroChem* **2014**, *1*, 1647–1655.

(31) Kajisa, T.; Sakata, T. Glucose-Responsive Hydrogel Electrode for Biocompatible Glucose Transistor. *Sci Technol Adv Mater* **2017**, *18*, 26–33.

(32) Matsumoto, A.; Sato, N.; Sakata, T.; Kataoka, K.; Miyahara, Y. Glucose-Sensitive Field Effect Transistor Using Totally Synthetic Compounds. *J. Solid State Electrochem.* **2009**, *13*, 165–170.

(33) Masuda, T.; Kajisa, T.; Akimoto, A. M.; Fujita, A.; Nagase, K.; Okano, T.; Sakata, T.; Yoshida, R. Dynamic Electrical Behaviour of a Thermoresponsive Polymer in Well-Defined Poly(N-Isopropylacrylamide)-Grafted Semiconductor Devices. *RSC Adv.* **2017**, *7*, 34517–34521.

(34) Edwards, J. O.; Sederstrom, R. J. The Thermodynamics of Ionization of Benzeneboronic Acid. *J. Phys. Chem.* **1961**, *65*, 862–863.

(35) Yurkevich, A. M.; Kolodkina, I. I.; Ivanova, E. A.; Pichuzhkina, E. I. Study of the Interaction of Polyols with Polymers Containing N-Substituted [(4-Boronophenyl) Methyl]-Ammonio Groups. *Carbohydr. Res.* **1975**, *43*, 215–224.

(36) Furikado, Y.; Nagahata, T.; Okamoto, T.; Sugaya, T.; Iwatsuki, S.; Inamo, M.; Takagi, H. D.; Odani, A.; Ishihara, K. Universal Reaction Mechanism of Boronic Acids with Diols in Aqueous Solution: Kinetics and the Basic Concept of a Conditional Formation Constant. *Chem. Eur. J.* **2014**, *20*, 13194–13202.

(37) Maekawa, Y.; Shibuta, Y.; Sakata, T. Charge Behaviors around Oxide Device/Pseudo-Physiological Solution Interface with Molecular Dynamic Simulations. *Jpn. J. Appl. Phys.* **2013**, *52*, 127001.

(38) Maekawa, Y.; Shibuta, Y.; Sakata, T. Distinctive Potential Behavior at the Oxidized Surface of a Semiconductor Device in a Concentrated Aqueous Salt Solution. *ChemElectroChem* **2014**, *1*, 1516–1524.

(39) Lowe, B.; Maekawa, Y.; Shibuta, Y.; Sakata, T.; Skylaris, C.-K.; Green, N. Dynamic Behaviour of the Silica-Water-Bio Electrical Double Layer in the Presence of a Divalent Electrolyte. *Phys. Chem. Chem. Phys.* **2017**, *19*, 2687–2701.

(40) Lowe, B. M.; Skylaris, C.-K.; Green, N. G.; Shibuta, Y.; Sakata, T. Molecular Dynamics Simulation of Potentiometric Sensor Response: The Effect of Biomolecules, Surface Morphology and Surface Charge. *Nanoscale* **2018**, *10*, 8650–8666.

(41) Kaiser, H. Die Berechnung Der Nachweisempfindlichkeit. *Spectrochim. Acta* **1947**, *3*, 40–67.

(42) Sakata, T.; Miyahara, Y. Detection of DNA Recognition Events Using Multi-Well Field Effect Devices. *Biosens. Bioelectron.* **2005**, *21*, 827–832.

(43) Sakata, T.; Miyahara, Y. DNA Sequencing Based on Intrinsic Molecular Charges. *Angew. Chem. Int. Ed. Engl.* **2006**, *45*, 2225–2228.

(44) Palazzo, G.; De Tullio, D.; Magliulo, M.; Mallardi, A.; Intranuovo, F.; Mulla, M. Y.; Favia, P.; Vikholm‐Lundin, I.; Torsi, L. Detection Beyond Debye's Length with an Electrolyte‐Gated Organic Field‐Effect Transistor. *Adv. Mater.* **2015**, *27*, 911–916.

(45) Debye, P.; Hückel, E. Zur Theorie Der Elektrolyte. I. Gefrierpunktserniedrigung Und Verwandte Erscheinungen. *Phys. Zeit.* **1923**, *24*, 185−206.

(46) Sasaki, S.; Ooya, T.; Kitayama, Y.; Takeuchi, T. Molecularly Imprinted Protein Recognition Thin Films Constructed by Controlled/Living Radical Polymerization. *J. Biosci. Bioeng.* **2015**, *119*, 200–205.

(47) Kamon, Y.; Matsuura, R.; Kitayama, Y.; Ooya, T.; Takeuchi, T. Precisely Controlled Molecular Imprinting of Glutathione-S-Transferase by Orientated Template Immobilization Using Specific Interaction with an Anchored Ligand on a Gold Substrate. *Polym. Chem.* **2014**, *5*, 4764–4771.

(48) Sakata, T.; Kamahori, M.; Miyahara, Y. DNA Analysis Chip Based on Field-Effect Transistors. *Jpn. J. Appl. Phys.* **2005**, *44*, 2854–2859.

Figure Captions

Figure 1 (a) Schematic diagram of GluMIP-coated gate FET. The Au electrode with the GluMIP interface was extended from the gate of FET. (b) Chemical structure of copolymerized glucose-imprinted MIP hydrogel.

Figure 2 Changes in capacitance of GluMIP interface upon adding glucose in the range from 10 μM to 10 mM. The GluMIP membrane was coated on the Au electrode.

Figure 3 Changes in V_G of GluMIP-coated gate FET at various pHs (100 mM sodium phosphate buffer). V_G was determined at a constant I_D of 1 mA and V_D of 2.5 V.

Figure 4 ΔV_T upon adding glucose at 0 (black), 10 μM (red), 100 μM (blue), 1 mM (green), and 10 mM (orange) analyzed from V_G-I_D electrical characteristics.

Figure 5 ΔV_{out} of GluMIP-coated FET upon adding sugars at 1 mM in turn. Each sugar was added at times indicated by arrows. (Glu, glucose; Fru, fructose; Suc, sucrose)

Figure 6 ΔV_{out} of GluMIP-coated FET upon adding sugars (red, glucose; blue, fructose; green, sucrose). Each sugar was added at time indicated by arrows in the range from 10 μM to 20 mM. As a control sensor, NIP-coated FET was prepared (black).

Figure 7 ΔV_{out} of GluMIP-coated FET for each sugar concentration (red, glucose; blue, fructose; green, sucrose). (a) The plots were approximated by the Langmuir absorption isotherm. (b) ΔV_{out} values were plotted for the changes in semilogarithmic sugar concentrations. The slope of an approximately straight line means the detection sensitivity for a sugar.

Table 1 Potentiometric Langmuir isotherm parameters of GluMIP-coated FET for glucose, fructose, and sucrose.

Table of Contents (TOC)

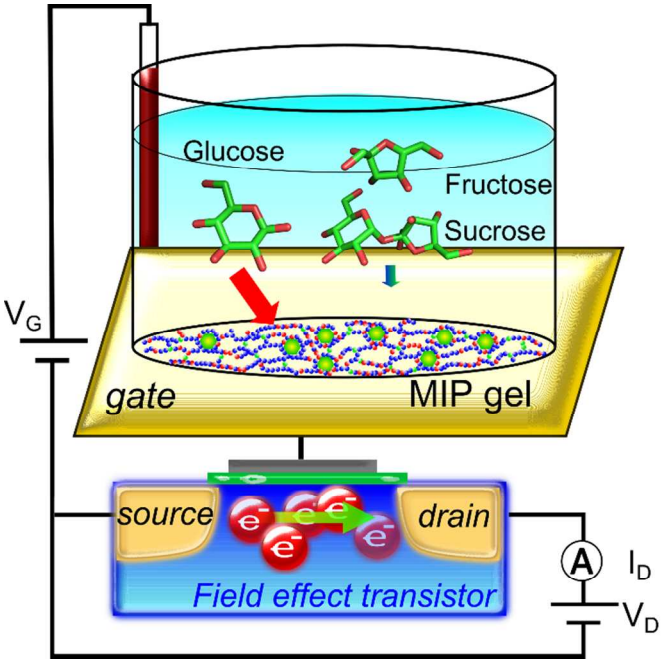

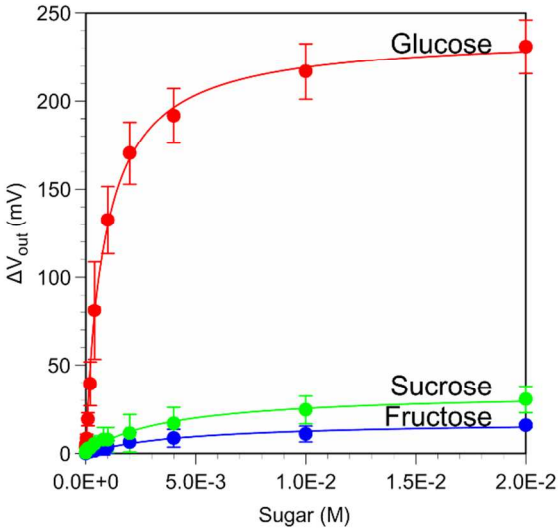

(a)

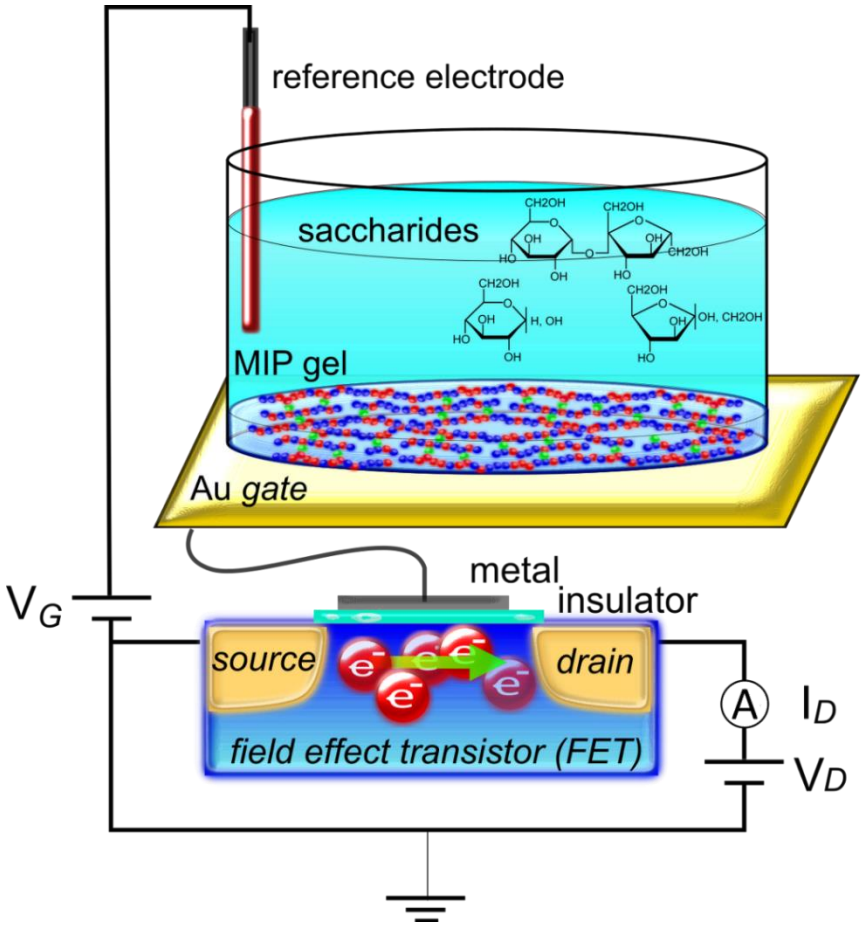
reference electrode
saccharides
MIP gel
Au gate
metal
insulator
source
drain
field effect transistor (FET)
V_G
A
I_D
V_D

(b)

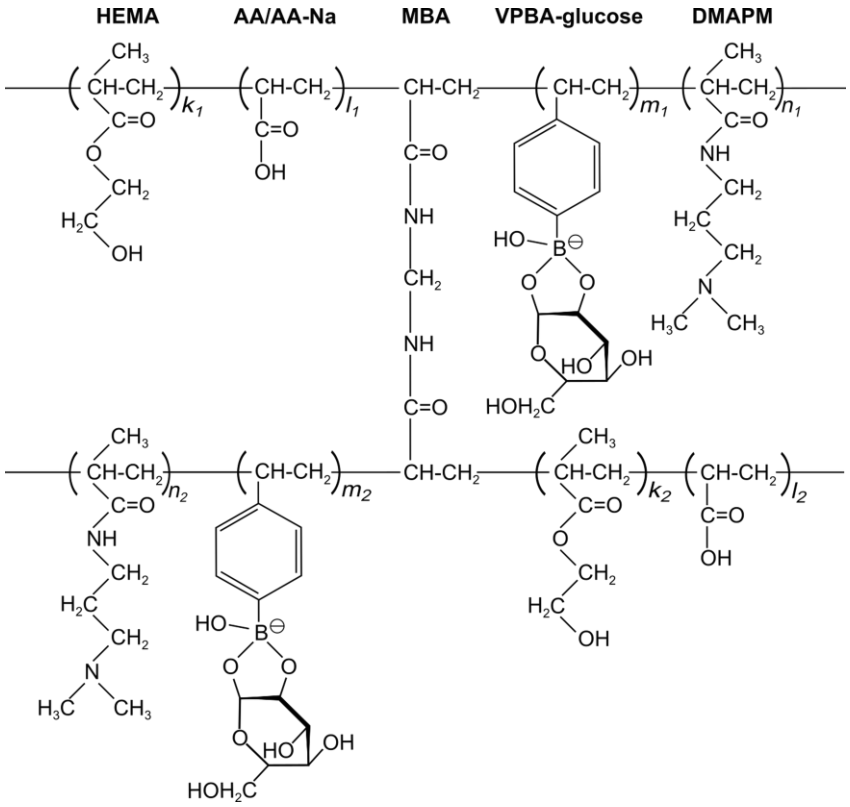
HEMA
AA/AA-Na
MBA
VPBA-glucose
DMAPM

Figure 1

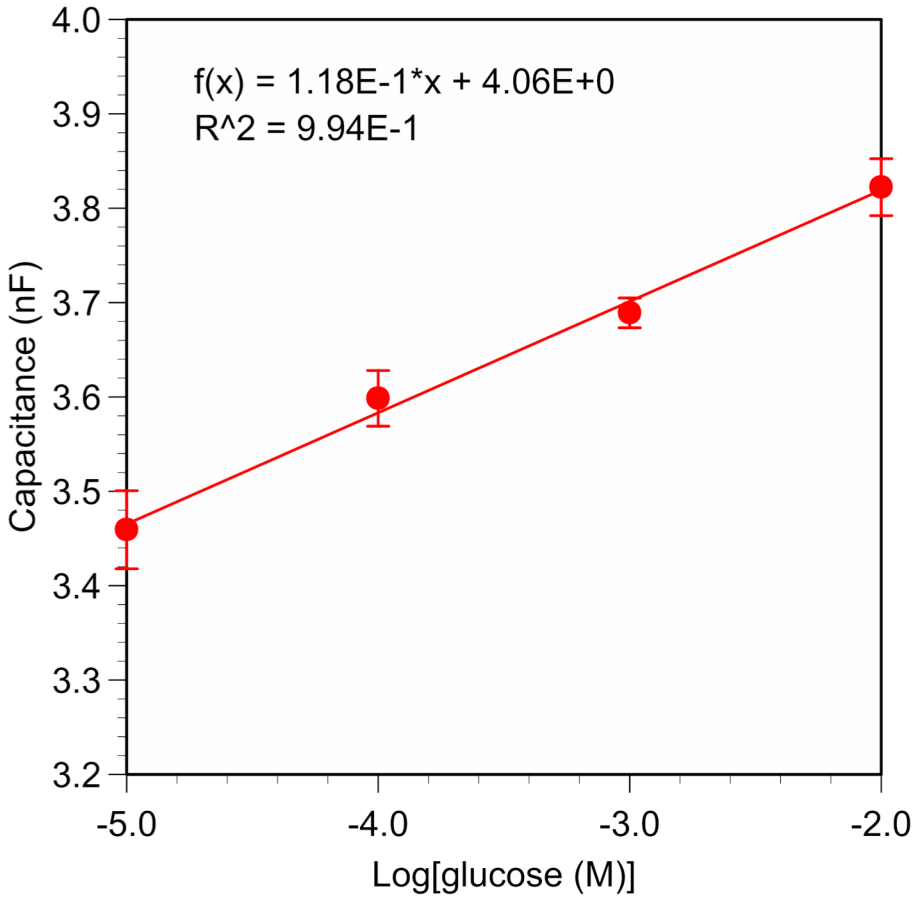
f(x) = 1.18E-1*x + 4.06E+0
R^2 = 9.94E-1
Capacitance (nF)
4.0
3.9
3.8
3.7
3.6
3.5
3.4
3.3
3.2
-5.0
-4.0
-3.0
-2.0
Log[glucose (M)]

Figure 2

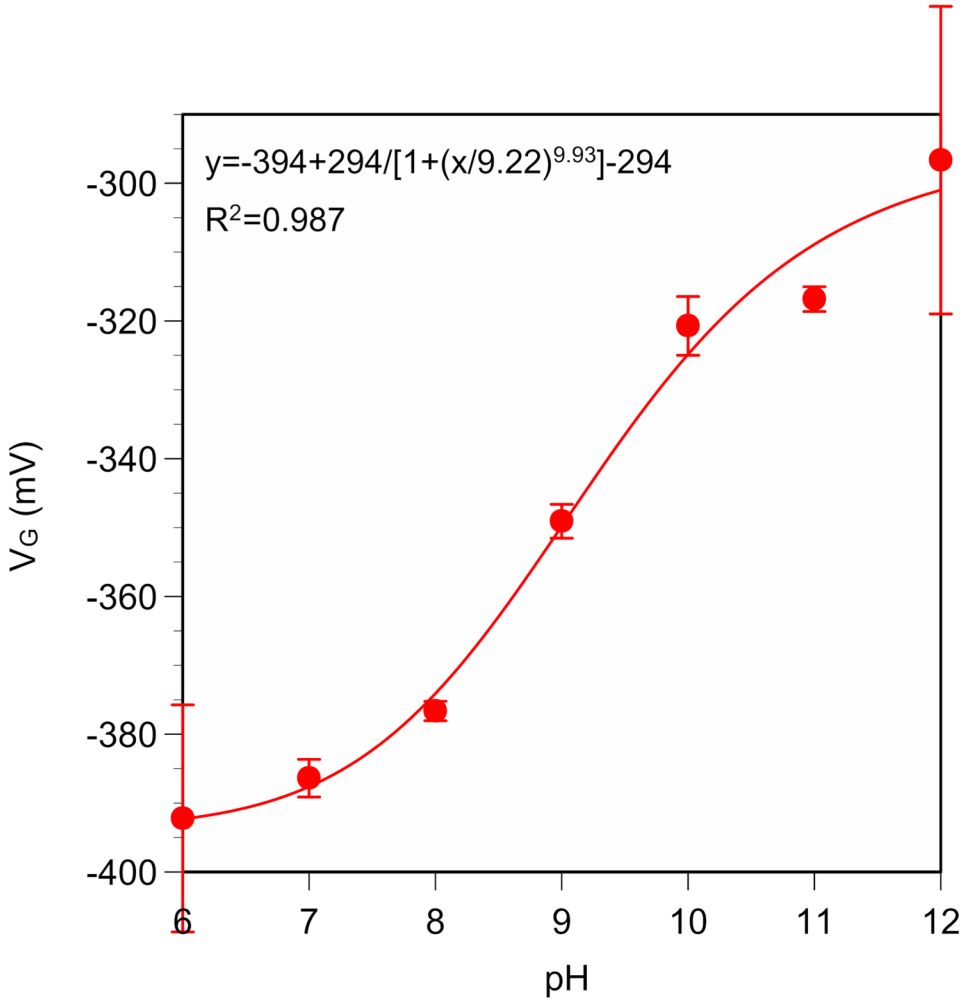
y=-394+294/[1+(x/9.22)^9.93]-294
R^2=0.987
-300
-320
-340
-360
-380
-400
V_G (mV)
6
7
8
9
10
11
12
pH

Figure 3

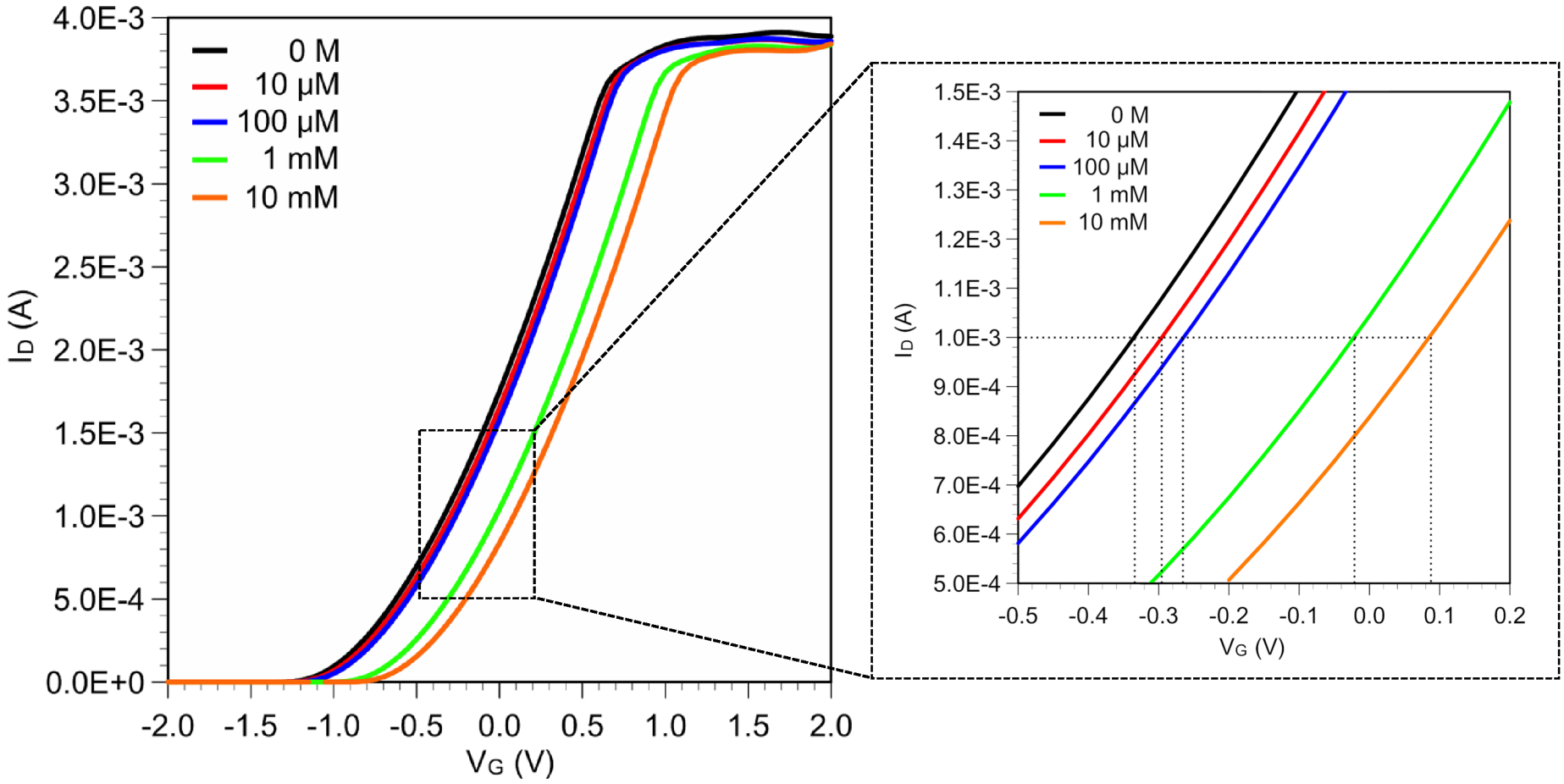

revised Figure 4

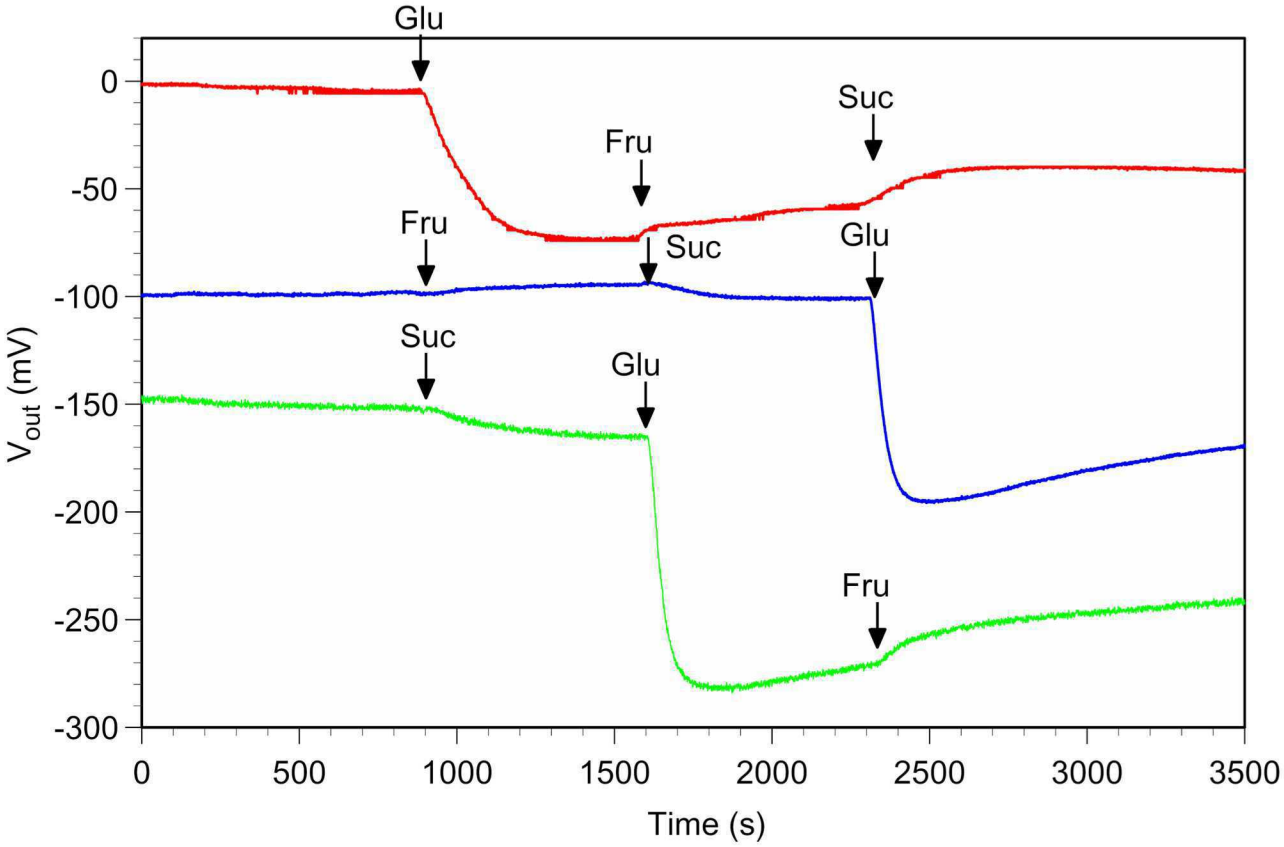
Glu
Fru
Suc
Fru
Suc
Glu
Suc
Glu
Fru
0
-50
-100
-150
-200
-250
-300
V_{out} (mV)
0
500
1000
1500
2000
2500
3000
3500
Time (s)

Figure 5

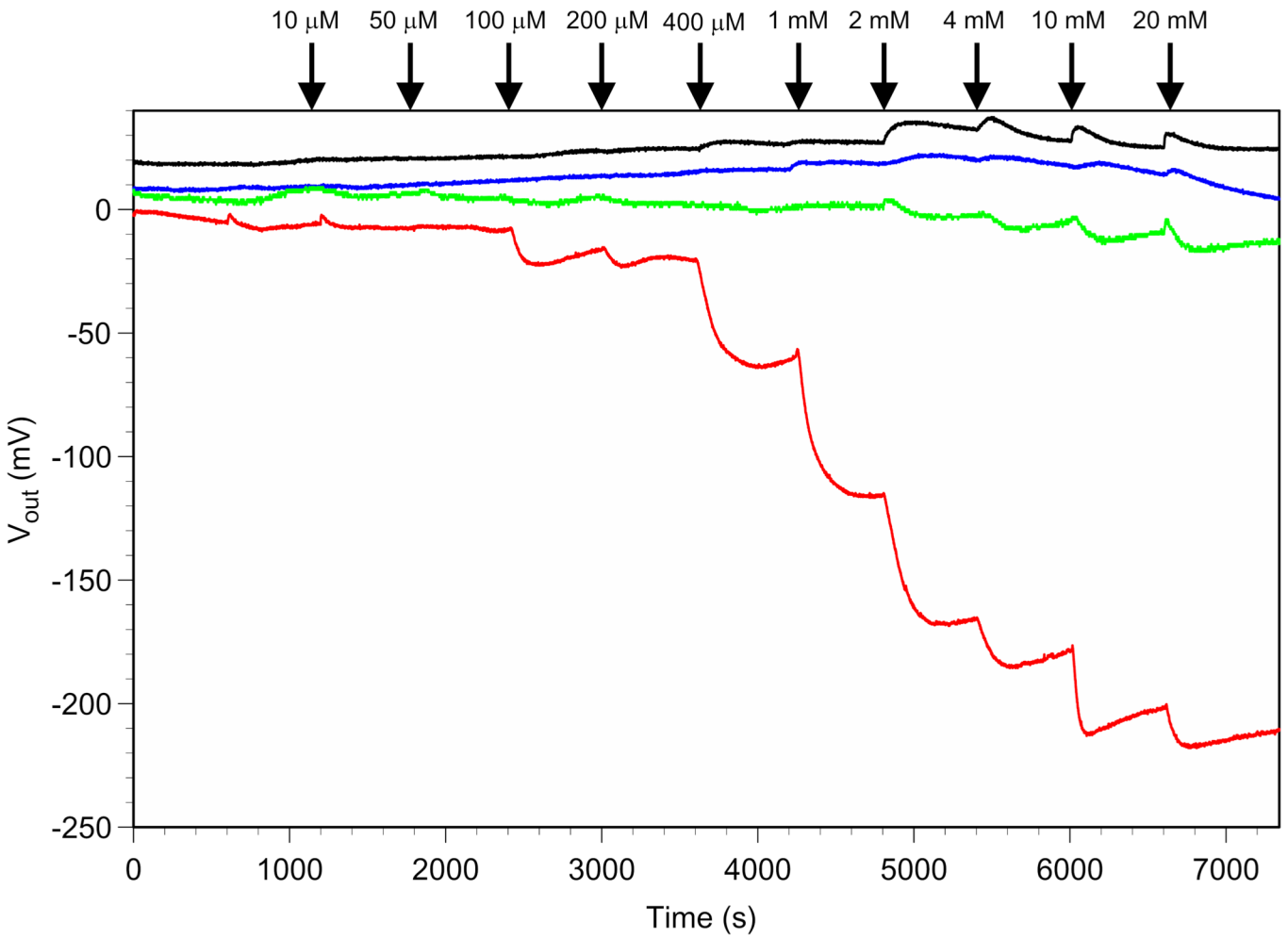
10 μM
50 μM
100 μM
200 μM
400 μM
1 mM
2 mM
4 mM
10 mM
20 mM
0
-50
-100
-150
-200
-250
V_{out} (mV)
0
1000
2000
3000
4000
5000
6000
7000
Time (s)

Figure 6

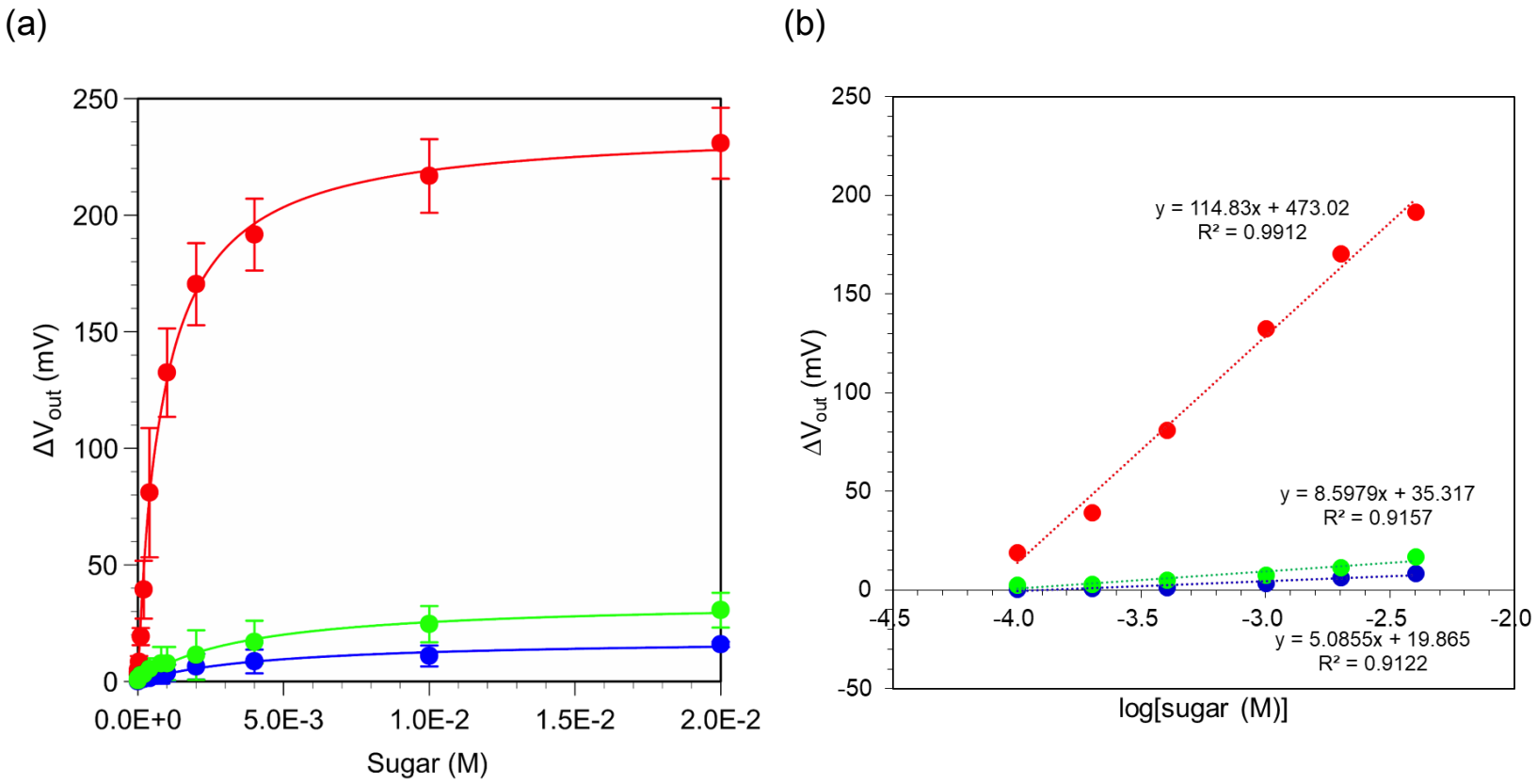

revised Figure 7

sugar	ΔV_{out} (mV)	K_a (M^{-1})	R^2
glucose	238	1192	0.998
fructose	18	212	0.984
sucrose	35	272	0.986

Table 1